



# Boosting Photocatalytic Hydrogen Production from Water in Poly(heptazine imides): The Role of the Mg<sup>2+</sup>-OH<sub>2</sub>-Pt Interface

Gabriel A. A. Diab, <sup>1,2\*</sup> Izadora F. Reis, <sup>2</sup> Rayse M. Ferreira, <sup>2</sup> Sara Stolfi, <sup>3,4</sup> Vitor G. S. Pastana, <sup>2</sup> Marcos A. R. da Silva, <sup>2</sup> Piero Torelli, <sup>4</sup> Paolo Ghigna, <sup>3</sup> Bruna R. Serino, <sup>2</sup> Viola Duppel, <sup>1</sup> Maurizio Fagnoni, <sup>3</sup> Sebastian Bette, <sup>1</sup> Davide Ravelli, <sup>3</sup> Bettina V. Lotsch, <sup>1</sup> Ivo F. Teixeira <sup>2</sup>

# Resumo/Abstract (Helvética, tam. 12)

RESUMO - Em resposta à crise climática e à demanda por energia sustentável, o hidrogênio molecular desponta como pilar da transição rumo à neutralidade de carbono. Entre os métodos verdes, a evolução fotocatalítica de H<sub>2</sub> destaca-se por armazenar energia solar em ligações químicas. Neste estudo, relatamos o aprimoramento dessa evolução via incorporação de magnésio em nitreto de carbono semicristalino. No trabalho, demontramos que estruturas de Poli(Heptazina Imida) dopadas com Mg<sup>2+</sup> mostraram fotoatividade excepcional, alcançando taxas de até 6452  $\mu$ mol g<sup>-1</sup> h<sup>-1</sup> e AQY de ~6% sob luz visível. Análises combinadas de desempenho fotocatalítico e XANES *in situ* revelaram uma interação sinérgica entre íons Mg<sup>2+</sup> na PHI e cocatalisadores de Pt fotodepositados. Identificamos um domínio interfacial Mg<sup>2+</sup>—OH<sub>2</sub>—Pt próximo aos sítios ativos, essencial para a transferência de carga e aumento da eficiência. A dopagem com Mg<sup>2+</sup> mostra-se promissora para aplicação ampla em sistemas fotocatalíticos, com impacto relevante na produção sustentável de H<sub>2</sub>.

Palavras-chave: Reação de Evolução de Hidrogênio (HER); Nitretos de Carbono Cristalinos; Poli(Heptazina imidas); XANES in situ

ABSTRACT - In response to the climate crisis and growing demand for sustainable energy, molecular hydrogen has emerged as a key pillar in the transition toward carbon neutrality. Among green production routes, photocatalytic H<sub>2</sub> evolution stands out as a promising method for storing solar energy as chemical energy. Here, we report enhanced H<sub>2</sub> evolution *via* magnesium incorporation into semi-crystalline carbon nitride. Mg-doped poly(heptazine imide) (Mg-PHI) frameworks exhibited outstanding photoactivity, achieving H<sub>2</sub> evolution rates up to 6452 µmol g<sup>-1</sup> h<sup>-1</sup> and an AQY near 6% under visible light. A comprehensive analysis combining photocatalytic performance and *in situ* XANES revealed a cooperative synergy between Mg<sup>2+</sup> ions embedded in PHI and photodeposited Pt cocatalysts. We identified a Mg<sup>2+</sup>–OH<sub>2</sub>–Pt interfacial domain near active sites, which facilitates charge transfer and boosts H<sub>2</sub> evolution. These results highlight Mg<sup>2+</sup> doping as a promising strategy for broader application across photocatalytic systems, with strong potential to impact sustainable H<sub>2</sub> production.

Keywords: Hydrogen Evolution Reaction (HER); Crystalline Carbon Nitrides; Poly(Heptazine imides); in situ XANES

# Introduction

Molecular hydrogen (H<sub>2</sub>) is a key player in the energy transition towards carbon neutrality, serving as a versatile, green energy carrier. Despite its importance, hydrogen production is still heavily reliant on fossil fuels, contributing significantly to CO<sub>2</sub> emissions. (*I*) Cleaner alternatives, such as solar-driven photocatalysis, are thus being intensively pursued. In this field, carbon nitrides—particularly Poly(Heptazine-Imide) (PHI) materials—stand out due to their structural order, chemical stability, and favorable optoelectronic properties. (*2*, *3*) PHIs, unlike traditional polymeric carbon nitrides, are ionic frameworks requiring counterions for charge balance, offering greater flexibility for electronic tuning. (*4*, *5*) However, their performance is limited by rapid exciton recombination and

inefficient charge transfer, necessitating co-catalysts as Pt to improve water reduction kinetics. Even so, noble metals alone cannot efficiently cleave the H–OH bond, presenting further challenges. (6-8)

Recent studies have shown that hydrated alkali and alkaline-earth cations can polarize water molecules, enhancing reaction kinetics by facilitating proton transfer and stabilizing reaction intermediates—an effect scalable with the metal's hydration energy. (9, 10) Inspired by this, doping semiconductors with such cations has emerged as a promising strategy, although experimental validation has remained limited.

In this work, we explore  $Mg^{2+}$  incorporation into Na-PHI through ion exchange, investigating its impact on photocatalytic  $H_2$  evolution. Our results show that  $Mg^{2+}$ 

<sup>&</sup>lt;sup>1</sup>Nanochemistry Department, Max Planck Institute for Solid State Research, Heisenbergstraße 1, 70569 Stuttgart, Germany.

<sup>&</sup>lt;sup>2</sup>Department of Chemistry, Federal University of São Carlos, 13565-905, São Carlos, SP, Brazil.

<sup>&</sup>lt;sup>3</sup>Department of Chemistry, University of Pavia, viale Taramelli 12, 27100 Pavia, Italy.

<sup>&</sup>lt;sup>4</sup>TASC Laboratory, CNR-IOM, Istituto Officina dei Materiali, Trieste, 34149 Italy.



significantly enhances activity when paired with Pt cocatalysts. In situ XANES analysis reveals electronic changes in  $\mathrm{Mg^{2+}}$  only in the presence of Pt, confirming a critical synergistic interaction at the  $\mathrm{Mg^{2+}\text{-}OH_2\text{-}Pt}$  interface that underpins the observed enhancement.

# Experimental

Na-PHI synthesis

The synthesis of Sodium poly(heptazinic imide) – Na(PHI) was carried out *via* the ionothermal approach, where melamine was employed as the nitrogen-rich precursor and NaCl as directing salt.(*11*) Initially, a homogeneous solid mixture was obtained by grinding melamine with NaCl at a ratio of 1:10 (wt %) using a ball mill. The resulting fine powder was placed in an alumina crucible, loosely closed with a lid, and subjected to calcination at 600 °C for 4 h, with a heating rate of 2.3 ° min<sup>-1</sup>, under N<sub>2</sub> atmosphere (0.2 L min<sup>-1</sup>). Subsequently, the resulting strong yellowish product was washed with deionized water (DI) and dried overnight at 60 °C.

#### Cationic Exchange

The incorporation of  $Mg^{2+}$  cations was achieved through direct cation exchange in aqueous medium, allowing the replacement of  $Na^+$  ions within the PHI framework by the desired metal. This method consists of suspending Na-PHI in an aqueous solution containing a specific concentration of  $MgCl_2$  salt. It enables controlled insertion of the new cation which depends solely on the solution concentration.

For the preparation of Mg-PHI containing 5.5% of  $Mg^{2+}$  incorporated, 100 mg of Na-PHI was initially suspended in 2 mL of an aqueous  $MgCl_2 \cdot 6H_2O$  solution (5 M) (see **Table S1** for other concentrations). The mixture was then sonicated for 15 min, washed with DI and dried overnight at 60 °C. Other metals such as  $Li^+$  K $^+$  and  $Ca^{2+}$  were also introduced for comparison tests. For those, a fixed concentration of 1 M was employed, with the respective chloride salt serving as precursor.

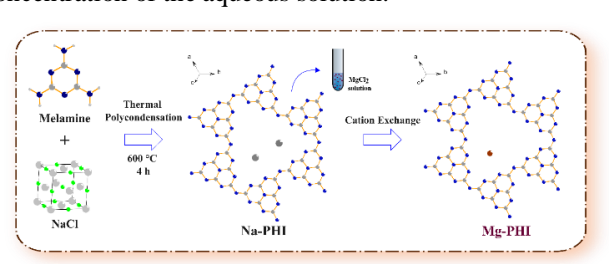
**Table 1.** Correlation of the MgCl<sub>2</sub> concentration for the obtention of Mg-PHI X% accompanied by the real loading of Na<sup>+</sup> and Mg<sup>2+</sup> measured by ICP-OES.

Label	$MgCl_2$ solution concentration (mol $L^{-1}$ )	Na <sup>+</sup> (Wt. %)	Mg <sup>2+</sup> (Wt. %)
Na-PHI	-	6.62	-
Mg-PHI 3%	0.05	5.78	2.66
Mg-PHI 4%	0.25	4.85	4.17
Mg-PHI 4.5%	2.5	3.77	4.58
Mg-PHI 5.5%	5.0	2.91	5.42

Results and DiscussionThe bottom-up fabrication of the PHI material was achieved through the thermal



polycondensation of melamine as a nitrogen rich precursor to obtain the polymeric backbone.(11, 12) Concerning the different PHI arrangements existing in literature, Nacontaining PHI (Na-PHI) was chosen due to its highly ordered arrangement and negatively charged framework, suitable for Mg<sup>2+</sup> incorporation and stabilization. In contrast to other approaches previously described, wherein the attainment of well-ordered 2D long-range heptazine units typically depends on a molten salt medium (such as eutectic mixtures of alkali salts, KSCN and others), our approach utilizes solely NaCl, which remains in the solid state during PHI formation (Scheme 1).(13-15) In the final ordered structure, the sodium cations introduced are hosted near the bridging imide nitrogen atoms, serving as a counter-ion throughout the plane, conferring a long-range structural material, as evidenced by sharp peaks in the PXRD pattern (Fig. 1a). The sodium cations present in the structure can be readily replaced by magnesium through a simple ion exchange procedure in an aqueous solution.(16, 17) This approach provides a controlled insertion of Mg<sup>2+</sup> within the PHI scaffold, allowing a systematic investigation of the influence of Mg2+ centers by evaluating the chemical and photocatalytic properties of the material containing when different amounts of the metal are incorporated. Its loading was monitored via ICP-OES, Table 1, proving that this process follow a quadratic trend and is governed by the concentration of the aqueous solution.



**Scheme 1.** Illustrative representation of the Mg-PHI fabrication. Initially, the original Na-PHI is formed by the bottom-up synthesis using melamine and NaCl as starting point. Once the Na-PHI is formed, the Na<sup>+</sup> cations are replaced by Mg<sup>2+</sup> through a cation exchange in aqueous medium. Color map: light grey – carbon, green – chlorine, blue – nitrogen, white – hydrogen, dark grey – sodium, wine – magnesium.

The crystalline structures of both synthesized materials were analyzed using PXRD to identify potential structural changes resulting from the incorporation of Mg<sup>2+</sup> ions, as well as the formation of oxygenated magnesium species was also considered. The diffraction patterns of the produced materials are shown in **Fig. 1a**. Its periodic arrangement along the plane, indicated by the 100 peak (corresponding to 10.8 Å distance) reflects the ordered alignment of heptazine units in the sheet dimension.(*12*) Additionally, its out-of-plane stacking is described by the 001 reflection at approximately 26.3° and 26.8° for Na-PHI and Mg-PHI 5.5



%, respectively. Indicating a slight shrinking of the interlayer distance caused by the Na<sup>+</sup> replacement, which is consistent since Mg<sup>2+</sup> ions has smaller ionic radii.(9) As a typical feature for PHIs synthesized by the bottom-up approach, this region is characterized by a series of overlapping and low-intensity signals, which suggests poor packing of the layers.(12) This disordered stacking may be attributed to a random arrangement of the sheets along the stacking direction.(18)

Essentially, the material exchanged with Mg did not exhibit drastic changes in the crystalline lattice. Reflections attributed to MgO and Mg(OH)<sub>2</sub> are absent in the fresh material. The final spatial arrangement of the PHI seems to be preserved during the exchange process. Nevertheless, the replacement of Na<sup>+</sup> by Mg<sup>2+</sup> resulted in a slight widening of the diffraction plane 100, while the diffraction peak 110 became more prominent.

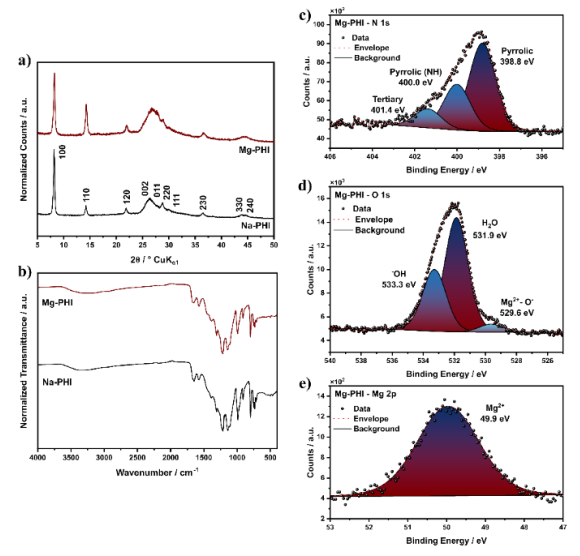


**Figure 1.** Comparative analysis of Na-PHI and Mg-PHI 5.5% w/w based on: a) PXRD pattern; b) FT-IR spectra and c-e) high resolution XPS spectra of N 1s, O 1s and Mg 2p regions obtained for Mg-PHI 5.5% w/w.

Furthermore, FT-IR and XPS analyses were performed in order to verify possible changes in the chemical structure of the support after cation exchange (displayed in the **Fig. 1b** and **Fig. 1c-e**). Initially, through the FR-IR, the distinctive binding framework of Na-PHI can be highlighted, characterized by its heteroaromatic units interlinked *via* negatively charged bridge nitrogen species. The metal presence, interconnected to the bridge negative nitrogen centers, is evidenced by the band at 980 cm<sup>-1</sup>. This signal is preserved for Mg-PHI, confirming the presence of cations in the network even after the cation exchange. Remarkably, the chemical backbone of the PHI did not undergo any significant changes during the cationic exchange. A change in the intensity ratio between the bands in the 1600–1800 cm<sup>-1</sup> region, characteristic of *v* N-H groups, suggests the



possibility of slight and incomplete protonation of some negatively charged bridge nitrogen following Mg<sup>2+</sup> insertion.(19)

Regarding the XPS analysis, the high resolution regions corresponding to O 1s, N 1s, and Mg 2p (**Fig. 1c–e**) were examined for the sample with the highest Mg content. Initially, the presence of the Mg sites as a single band of low intensity at 50 eV.(20, 21) The N 1s region displayed basically the characteristic signals associated with PHI-type structures, with no significant differences compared to data reported for Na-PHI.(22, 23)

In the O 1s region, the spectrum displays signals attributed to surface hydroxyl groups (531.9 eV) and physisorbed water molecules (533.3 eV).(20, 24) A signal emerges at lower binding energy (531.9 eV), which can be attributed to oxygen species from a hydration shell interacting with Mg sites within the PHI pores. This signal is potentially originated from Mg(OH)<sub>2</sub> or Mg-OH<sub>2</sub> species.

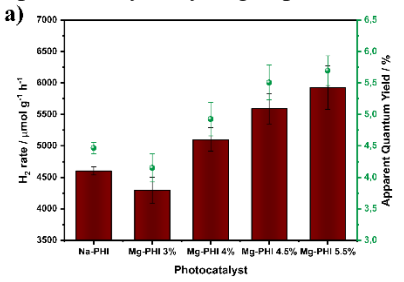
# **Photocatalytic Experiments**

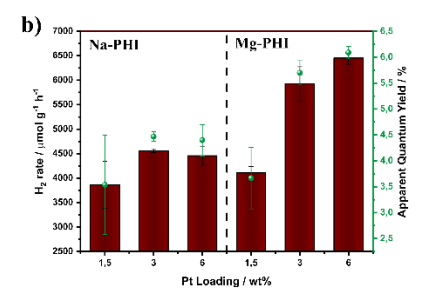
Overall, as verified from the previous analyses, the cationic replacement of  $Na^+$  by  $Mg^{2+}$  in the PHI structure did not significantly affect the structural, chemical and optoelectronic properties of the starting material. Initially, to evaluate the quantitative impact of  $Mg^{2+}$  on photoactivity, reactions for  $H_2$  evolution were performed using materials containing different amounts of Mg. The results obtained are shown on **Fig. 2a**. The introduction of 3% Mg into the network does not produce significant changes in the amount of hydrogen produced compared to Na-PHI. However, starting from 4% Mg, a linear increase in the activity of the material is observed, reaching its peak in production for the material with the highest Mg loading (5.5 %), achieving 5928  $\mu$ mol  $g^{-1}$   $h^{-1}$ , around 1.3-fold higher compared to the original material.

Given the considerable effect of magnesium presence in the network, the system behavior was studied by varying the platinum loading photodeposited on Mg-PHI with the best performance for HER, i.e., with structure saturated with Mg<sup>2+</sup>. The same approach was applied to Na-PHI as comparison. As shown in Fig. 2b, Mg-PHI consistently exhibited superior hydrogen evolution activity compared to Na-PHI across all platinum loadings. Notably, for Na-PHI, increasing the amount of photodeposited platinum had little to no effect on the H<sub>2</sub> production rate, indicating that for this system, the catalytic performance is not governed by cocatalyst availability. This observation also suggests the existence of a threshold in co-catalyst deposition beyond which no further enhancement in H<sub>2</sub> evolution is achieved. However, the opposite behavior was observed for Mgcontaining samples. For these materials, the observed trend was quite similar to the study with different amounts of Mg, i.e., increasing proportionally to the added amount, yielding the maximum value of 6542  $\mu$ mol g<sup>-1</sup> h<sup>-1</sup> H<sub>2</sub> production rate



when using Mg-PHI 5.5% and 6% w/w of photodeposited Pt co-catalyst. Since the enhancement in  $H_2$  evolution rate is observed exclusively in the concomitant presence of both the alkaline-earth metal and the Pt co-catalyst, their coexistence gives rise to a synergistic interaction that facilitates photocatalytic hydrogen production.





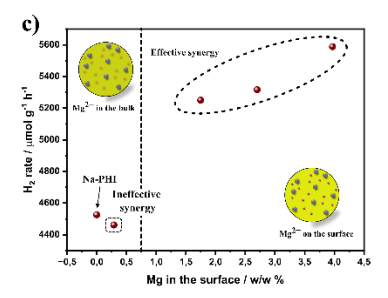


**Figure 2.** Photocatalytic  $H_2$  evolution results under visible light irradiation (410 nm, 50 W): a) varying the  $Mg^{2+}$  using a fixed 3% Pt loading and b) influence of Pt loading for Na-PHI and Mg-PHI (5.5 %); c) estimation of surface-accessible  $Mg^{2+}$  species onto the PHI framework.

Considering that the photodeposition of photoactive Pt nanoparticles occurs primarily on the surface of PHI, it is reasonable to assume that the supportive role of Mg<sup>2+</sup> is effective only for cations positioned near the co-catalyst, *i.e.*, on the surface of the material. Based on this, the lack of observed synergy between the alkaline earth metal and the co-catalyst in the case of Mg-PHI 3% can be attributed to the fact that, for this composition, the Mg<sup>2+</sup> ions are predominantly located within the bulk of the framework, and therefore not available at the surface to promote the interfacial interaction herein proposed.

Although it is reasonable to argue that the absence of synergy might simply be due to the low concentration of Mg<sup>2+</sup>, insufficient to establish an effective interface, which is promoted by higher amounts of Mg<sup>2+</sup>. This possibility can



be ruled out by adding externally the same amount of  $Mg^{2+}$  in solution during the reaction using Na-PHI. The result obtained showed a significative increase in the hydrogen evolution rate from 4602 to 7235  $\mu$ mol g<sup>-1</sup> h<sup>-1</sup>, indicating that the synergistic effect does occur for the same  $Mg^{2+}$  concentration, but only when the ions are available near the active interface.

In this scenario, Mg<sup>2+</sup> ions in solution are expected to localize within the Helmholtz layer, *i.e.*, at an ideal proximity to the co-catalyst nanoparticles to establish the Mg<sup>2+</sup>–OH<sub>2</sub>–Pt interaction.

Based on these results, we could roughly estimate the amount of superficial  $Mg^{2+}$  through a simple calculation, assuming that the substitution sites are initially formed from the material's bulk towards the surface. Thus, the simple subtraction of the quantitative amount of  $Mg^{2+}$  incorporated by the remaining sodium content, divided by 2 (due to charge balance), provides an estimate of the amount of superficial Mg present. Surprisingly, the results demonstrate that effective superficial Mg only appears after the insertion of 4% w/w of  $Mg^{2+}$ . From this point onward,  $H_2$  evolution drastically increases (**Fig. 2c**), reinforcing that the proximity between  $Mg^{2+}$  atoms and the co-catalyst is essential for the synergistic effect observed in the reaction.

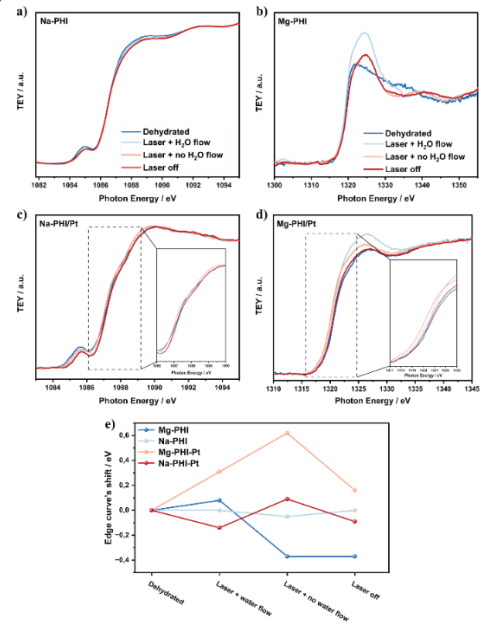


**Figure 3.** *In situ* XANES of the K edge window spectra of: a and c) Na and b and d) Mg metals of the photocatalysts without (upper panels) and with (lower panel) Pt co-catalyst under simulated reaction conditions followed by e) the respective shift of the K edge curve plotted according to each analysis condition. TEY: Total Electron Yield.

For a more in-depth understanding of the electronic influence of Mg<sup>2+</sup> and Na<sup>+</sup> cations on the photocatalytic system, *in situ* XANES experiments were conducted simulating the reactional conditions (**Fig. 3**). Both PHI



materials based on Na and Mg were compared in the presence and absence of Pt. Initially, the influence of water presence in the local structure was considered by performing a measurement on the material completely dried, *i.e.*, previously dehydrated at 250 °C (dark blue lines). Afterwards, the materials were directly photoexcited using a purple laser (408.63 nm, 40 mW), while simultaneously introducing a water flow into the system (light blue lines). This experiment enables a direct visualization of possible alterations in the electronic density, as well as the local symmetry, of the studied metal, caused by the electron transfer followed by reduction of protons.

Initially, reference measurements were taken for the materials without the Pt co-catalyst to evaluate the natural response of the studied metal edges under the given conditions. At the Na K-edge (Fig. 3a), illumination of the sample in flowing H2O causes a small decrease of the preedge peak at ca. 1085 eV, which is in turn due to Na  $1s \rightarrow 3s$ transition.(25) These transitions are dipole forbidden, but can turn into allowed ones if the local symmetry of Na is not strictly centro-symmetric; a decrease in intensity of this feature can be attributed to an increase of the occupation of Na 3s orbitals and/or to a more ordered local chemical environment around the Na sites, which increases the symmetry. Both these effects can be related to the adsorption of water on the Na sites. It is important to note that these changes in intensity are not reversed, neither by switching the laser off, nor interrupting the water flow, suggesting that H<sub>2</sub>O adsorption is strong. Other minor changes are detected at ca. 1088 eV, where the dipole allowed Na  $1s \rightarrow 3p$  transitions are found.(25) Also in this case, a largely non-reversible decrease in intensity is found, which can be likewise attributed to water adsorption, resulting in an increase of the occupation of Na 3p states. For the Mg K-edge (Fig. 3b), a marked increase in intensity of the main edge peak is found by flowing water under illumination, which can be partially reversed by stopping the H<sub>2</sub>O flow. Again, this variation in intensity is attributed to water adsorption, in agreement with previous literature:(26) the larger changes compared to the Na-containing material reveal that coordination of water around Mg cations has a greater impact on the local electronic density compared to Na.

For Na-PHI with photodeposited platinum co-catalyst (Fig. 3c), two distinct features are detected at the Na K-edge: i) a decrease in intensity of the pre-edge peak as discussed above, and ii) a shift of the edge absorption energy to a lower energy (by 0.15 eV, as better evidenced in the inset). For the material containing Mg in the presence of platinum (Fig. 3d), an increase in intensity of the main edge peak is again detected, but to a lower extent than in the previous case. Additionally, a shift of the edge energy position towards lower energy is revealed under illumination and in flowing water. As evidenced by the



inset, which shows the edge energy region on an enlarged scale, such shift amounts to 0.57 eV, almost four times larger than for sodium. After exposing the samples to these conditions, the water flow was interrupted, and the laser was switched off. Thereby, it was possible to observe the progressive return of the edge to its initial position, the most marked shift being produced by stopping the illumination, after having stopped the water flow.

We note that the edge energy position is a measure of the binding energy of the 1s electrons. This is due to the Coulomb interaction between such electrons and the nucleus, and it is in turn modulated by all the outer (valence) electrons. The larger the shielding, the lower the binding energy and, therefore, the lower the edge energy position. Thus, a shift of the edge towards lower energies is a clear indication of an increase in the electron density around Na and Mg, which reveals a decrease in the charge state. This effect is significantly larger for Mg than for Na and it is detected only in the presence of Pt (**Fig. 3e**).

In summary, a mechanism of the synergistic effect is proposed in **Fig. 4**. The XANES results in *in situ* conditions indicate that: i) Mg<sup>2+</sup> and Na<sup>+</sup> are preferential sites for water adsorption, and ii) a collaborative effect between Na<sup>+</sup>/Mg<sup>2+</sup> centers on the PHI framework and the Pt nanoparticles (acting as co-catalyst) operates, in which the synergy is more pronounced in magnesium-containing samples. These results support the hypothesis of a collaborative interaction between the alkali/alkaline-earth metals exchanged in the PHI structure and the noble metal, with the electron transfer from the co-catalyst to water facilitated by the alkali and alkaline-earth metals.

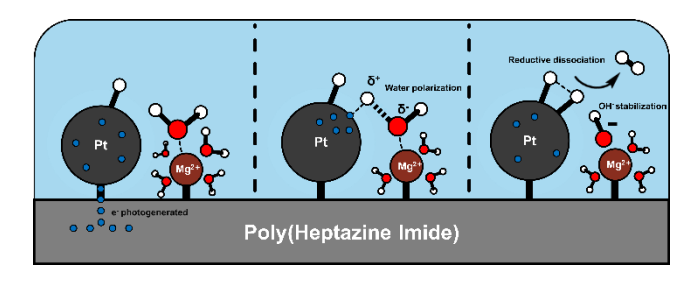


**Figure 4.** Proposed mechanism illustrating the collaborative contribution of the  $Mg^{2+}$  centers toward water polarization, promoting the facilitated proton transfer onto the Pt surface.

### Conclusions

In this study, we developed a simple method for introducing magnesium into the Na-PHI scaffold *via* controlled cation exchange in aqueous solution. Characterization confirmed successful Mg incorporation, leading to a significant improvement in photocatalytic H<sub>2</sub> evolution. Higher Mg loadings (>4% w/w) resulted in increased hydrogen production, with a linear enhancement at higher levels. A similar trend was observed with Pt nanoparticle photodeposition on Mg-exchanged PHI,



demonstrating a synergistic effect between Mg<sup>2+</sup> and Pt. *In situ* XANES confirmed the key role of the Mg<sup>2+</sup>-OH<sub>2</sub>-Pt interface. The results highlight that Na<sup>+</sup> and Mg<sup>2+</sup> act as preferential sites for water adsorption and facilitate proton transfer to Pt, boosting photoactivity. This work underscores the importance of interfacial interactions between Mg<sup>2+</sup> and Pt in enhancing photocatalytic performance. The Mg doping strategy offers a promising path for further improving AQY and can be extended to other photocatalytic systems, contributing to advances in sustainable hydrogen production.

# Acknowledge

This research was financially supported by the Brazilian funding agencies CAPES, CNPq, FINEP and FAPESP. The authors acknowledge support from Max-Planck-Gesellschaft, Deutsche Forschungsgemeinschaft via the Cluster of Excellence e-conversion, and the European Union's Horizon Europe program (project CATART). SS acknowledges a Ph.D. grant from the CATART project. We also acknowledge support from UniPV and MUR through the 'Departments of Excellence' program.

#### References

- G. A. A. Diab et al., A Solar to Chemical Strategy: Green Hydrogen as a Means, Not an End. Global Challenges n/a, 2300185.
- X. Wang et al., A metal-free polymeric photocatalyst for hydrogen production from water under visible light. Nature Materials 8, 76-80 (2009).
- M. Melchionna, P. Fornasiero, Updates on the Roadmap for Photocatalysis. ACS Catalysis 10, 5493-5501 (2020).
- S. Oleksandr, A. Markus, W. Xinchen, Eds., Carbon Nitrides (De Gruyter, Berlin, Boston, 2023).
- G. Zhang et al., Enhanced photocatalytic H2 production independent of exciton dissociation in crystalline carbon nitride. Applied Catalysis B: Environmental 338, 123049 (2023).
- J. Yuan et al., Crystallization, cyanamide defect and ion induction of carbon nitride: Exciton polarization dissociation, charge transfer and surface electron density for enhanced hydrogen evolution. Applied Catalysis B: Environmental 251, 206-212 (2019).
- C. M. Pelicano, H. Tong, Recent advances in cocatalyst engineering for solar-driven overall water splitting. *Applied Research* 3, e202300080 (2024).
- W. Yang et al., Electron Accumulation Induces Efficiency Bottleneck for Hydrogen Production in Carbon Nitride Photocatalysts. Journal of the American Chemical Society 141, 11219-11229 (2019).
- J. Mähler, I. Persson, A Study of the Hydration of the Alkali Metal Ions in Aqueous Solution. *Inorganic Chemistry* 51, 425-438 (2012).
- R. Subbaraman et al., Enhancing Hydrogen Evolution Activity in Water Splitting by Tailoring Li<sup>+</sup>-Ni(OH)<sub>2</sub>-Pt Interfaces. Science 334, 1256-1260 (2011)
- 11. I. F. Teixeira *et al.*, Improving hydrogen production for carbon-nitride-based materials: crystallinity, cyanimide



- groups and alkali metals in solution working synergistically. *Journal of Materials Chemistry A* **10**, 18156-18161 (2022).
- Z. Chen et al., "The Easier the Better" Preparation of Efficient Photocatalysts—Metastable Poly(heptazine imide) Salts. Advanced Materials 29, 1700555 (2017).
- J. Kröger et al., Morphology Control in 2D Carbon Nitrides: Impact of Particle Size on Optoelectronic Properties and Photocatalysis. Advanced Functional Materials 31, 2102468 (2021).
- D. Dontsova et al., Triazoles: A New Class of Precursors for the Synthesis of Negatively Charged Carbon Nitride Derivatives. Chemistry of Materials 27, 5170-5179 (2015).
- Z. Yang et al., Optimizing the Band Structure of Crystalline Potassium Poly(heptazine imide) for Enhanced Photocatalytic H2O2 Production and Pollutant Degradation. ACS ES&T Engineering 2, 2142-2149 (2022).
- J. Kröger et al., Conductivity Mechanism in Ionic 2D Carbon Nitrides: From Hydrated Ion Motion to Enhanced Photocatalysis. Advanced Materials 34, 2107061 (2022).
- A. Savateev, S. Pronkin, M. G. Willinger, M. Antonietti, D. Dontsova, Towards Organic Zeolites and Inclusion Catalysts:
   Heptazine Imide Salts Can Exchange Metal Cations in the Solid State. Chemistry An Asian Journal 12, 1517-1522 (2017).
- H. Schlomberg et al., Structural Insights into Poly(Heptazine Imides): A Light-Storing Carbon Nitride Material for Dark Photocatalysis. Chemistry of Materials 31, 7478-7486 (2019).
- V. Shvalagin et al., Simultaneous Photocatalytic Production of H2 and Acetal from Ethanol with Quantum Efficiency over 73% by Protonated Poly(heptazine imide) under Visible Light. ACS Catalysis 14, 14836-14854 (2024).
- J. T. Newberg et al., Formation of hydroxyl and water layers on MgO films studied with ambient pressure XPS. Surface Science 605, 89-94 (2011).
- Y. Ding et al., Preparation and Characterization of Magnesium Hydroxide Sulfate Hydrate Whiskers. Chemistry of Materials 12, 2845-2852 (2000).
- E. Alwin, W. Nowicki, R. Wojcieszak, M. Zieliński, M. Pietrowski, Elucidating the structure of the graphitic carbon nitride nanomaterials via X-ray photoelectron spectroscopy and X-ray powder diffraction techniques. *Dalton Transactions* 49, 12805-12813 (2020).
- M. A. R. da Silva et al., Simple and straightforward method to prepare highly dispersed Ni sites for selective nitrobenzene coupling to Azo/Azoxy compounds. Chemical Engineering Journal 460, 141068 (2023).
- 24. T. H. Nguyen et al., Single-step removal of arsenite ions from water through oxidation-coupled adsorption using Mn/Mg/Fe layered double hydroxide as catalyst and adsorbent. Chemosphere 295, 133370 (2022).
- G. J. McIntosh, A. Chan, Probing hydrogen bonding interactions and impurity intercalation in gibbsite using experimental and theoretical XANES spectroscopy. *Physical Chemistry Chemical Physics* 20, 24033-24044 (2018).
- F. Tavani et al., Caught while Dissolving: Revealing the Interfacial Solvation of the Mg2+ lons on the MgO Surface.
   ACS Applied Materials & Interfaces 14, 38370-38378 (2022).